

Highly ordered MnO₂ nanowire array thin films on Ti/Si substrate as an electrode for electrochemical capacitor

Cai-Ling Xu^a, Shu-Juan Bao^a, Ling-Bin Kong^b, Hua Li^a, Hu-Lin Li^{a,*}

^aCollege of Chemistry and Chemical Engineering, Lanzhou University, Lanzhou 730000, PR China

^bState Key Laboratory of Gansu Advanced Non-Ferrous Materials, Lanzhou University of Technology, Lanzhou 730050, PR China

Received 12 December 2005; received in revised form 18 January 2006; accepted 22 January 2006

Available online 14 March 2006

Abstract

AAO/Ti/Si substrate was successfully synthesized by a two-step electrochemical anodization of the aluminum film on the Ti/Si substrate and then used as template to grow nanowire arrays. The ordered MnO₂ nanowire arrays with about 40 nm diameters had been directly fabricated on AAO/Ti/Si substrate by direct current (DC) electrodeposition. The microstructure of the nanowire arrays was investigated by field-emission scanning electron microscopy, transmission electron microscopy and X-ray diffraction. Their electrochemical characterization was performed using cyclic voltammetry in 0.5 M Na₂SO₄ aqueous solution. The synthesized MnO₂ nanowires had amorphous nature until 400 °C. The deal capacitive behavior was obtained when the as-prepared sample was heat-treated at 200 °C. The specific capacitance of the electrode was about 254 F/g.

© 2006 Elsevier Inc. All rights reserved.

Keywords: MnO₂ nanowire arrays; AAO/Ti/Si substrate; Electrochemical capacitor

1. Introduction

Electrochemical capacitors are currently receiving considerable amount of attention because of their high power energy storage ability. It is well known that the most widely used active electrode materials are carbon [1,2], conducting polymers [3,4] and both noble [5–7] and transition metal oxides [8–26]. Among these candidates, MnO₂ has been considered to be the most attractive electrochemical capacitor materials in terms of its low cost, abundance and more environmental friendliness than other transition metal oxide systems [27].

Researches indicate that electrochemical characteristics of electrode materials are highly dependent on the grain size, texture, surface area, and morphology. The ordered, high surface area structure of electrode materials can enhance electrochemical characteristics. Martin and co-workers have demonstrated that high surface area nano-

wire array electrodes of SnO₂ and V₂O₅ have significantly improved rate capability compared with thin films of the same material [28–30]. Anodic aluminum oxide (AAO) template offers a promising route to synthesize a high surface area, ordered nanowire electrodes because of its advantages. Recently, amorphous manganese oxide nanowire arrays for high energy and power density electrodes were prepared by the AAO template method [31]. But this method is difficult to be used in practical purpose due to the fragility of the AAO template.

In this work, AAO films are successfully grown on Ti/Si substrate and this is first time it is used as a template to synthesize high surface area and ordered MnO₂ nanowire array electrode for electrochemical capacitors. This kind of template has unique electrodeposition properties and can bond well with the deposited materials. The electrochemical characterization of ordered MnO₂ nanowire arrays on Ti/Si substrate is performed by cyclic voltammetry in 0.5 M Na₂SO₄ aqueous solution using the nanowire array thin films as the working electrode. The nanowire array electrode consists of only electrochemically active material (MnO₂) and is fairly stable. The results of cyclic

*Corresponding author. Fax: +86 931 891 2582.

E-mail addresses: xucl01@163.com (C.-L. Xu), lihl@lzu.edu.cn (H.-L. Li).

voltammetry show that the specific capacitance of the electrode is about 254 F/g and has promising application in electrochemical capacitor.

2. Experimental

The highly pure Al film (99.999%, about 3.0 μm) was deposited on the p-type silicon substrate coated with a Ti (about 300 nm) film by radio frequency sputtering. The anodization was carried out in 0.3 M oxalic acid solution at room temperature, 40 V for about 40 nm pores in diameter. The resulting alumina film was etched away in 0.4 M H_3PO_4 , 0.2 M $\text{H}_2\text{Cr}_2\text{O}_4$ at 40 $^\circ\text{C}$ for 20 min, and the remaining aluminum was re-anodized under the same conditions until the metal film was fully oxidized. To remove the barrier layer, the anodization was continuously processed for 90–120 min. The details of removing the barrier layer will be reported in our later work.

The electrolyte was an aqueous solution of 0.5 M $\text{Mn}(\text{CH}_3\text{COO})_2$ for preparation of MnO_2 nanowire array thin films. Electrodeposition was carried out at room temperature, using a three-electrode potentiostatic control and direct current (DC) electrodeposition system with a saturated calomel electrode as reference electrode, a 1.0 cm \times 1.0 cm platinum plate as a counter electrode and the AAO/Ti/Si substrate as working electrode. The electrolysis was carried out at 1.0 V for 2 h.

After electrodeposition, the samples were immersed in 0.5 M NaOH solution for 1 h to remove the AAO on Ti/Si substrate. For electrochemical measurement, the nanowire arrays on Ti/Si substrate were used as working electrode, platinum foil with the same area of the working electrode and saturated calomel electrodes as the counter and reference electrodes, respectively.

The morphology of the porous anodic alumina film on Ti/Si substrate and nanowire arrays was examined by field emission scanning electron microscope (FESEM). Transmission electron microscopy (TEM) was used to characterize the morphology of nanowires. The crystalline structure of the samples was determined by X-ray diffraction (XRD). Thermo-gravimetric and different thermal analysis (TG–DTA) was performed for studying the change of synthesized sample with temperature. The electrochemical measurements of the samples were performed by means of a CHI660 electrochemical working station.

3. Results and discussion

After a two-step anodization in 0.3 M oxalic acid solution at room temperature, the resulting template has parallel pores with a fairly narrow size distribution, as shown in Fig. 1. Fig. 1a shows that the porous alumina structure has almost arranged the pore array with the average pore diameter about 40 nm, the interspaces about 60 nm, and pore densities about 10^{10} cm^{-2} . But their arrangement has lower order than AAO on bulk Al probably duo to small grain [32] and thin aluminum films

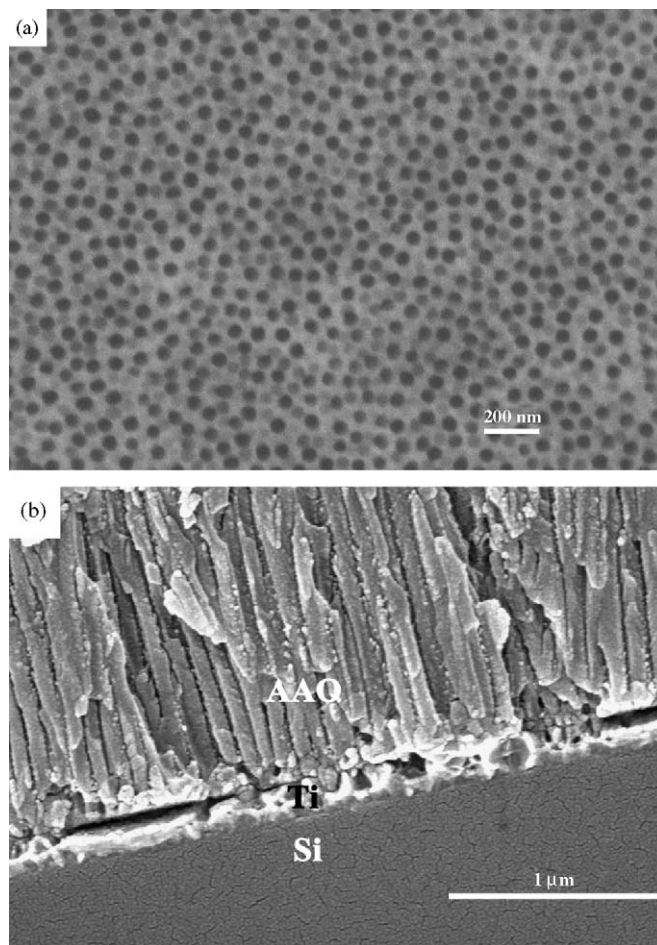


Fig. 1. FESEM images of an alumina template on a Ti/Si substrate created using a two-step anodization process in 0.3 M oxalic acid solution at room temperature: (a) top view, (b) side view.

[33]. From Fig. 1b, we can see that the thickness of the Ti adhesion layer is approximately 300 nm and not uniform because we cannot well control the zone of fracture of sample when it is breached for FESEM observation. The pores partly open to the Ti layer because of the short oxidation time. The oxide barrier layer can be completely removed by continuously prolonging the oxidation time for DC electrodeposition.

The FESEM image in Fig. 2 shows the surface view of MnO_2 nanowire arrays. From Fig. 2, we can find that many clusters protrude from the Ti/Si substrate which provide high surface area electrode. The clusters could result from the situation in which the nanowires are uncovered from the framework of the porous anodic alumina template but freestanding incompletely. When the porous anodic alumina template was dissolved away, the nanowires embedded in the template were released gradually and inclined to agglutinate together to minimize the system free energy. Fig. 2 also shows that the nanowires are abundant, uniform and well ordered in the large area. From Fig. 2 it can be estimated that the pore filling rate is above 90%, and some nanowires are lost from the electrode surface. The diameter and the length of the nanowires are

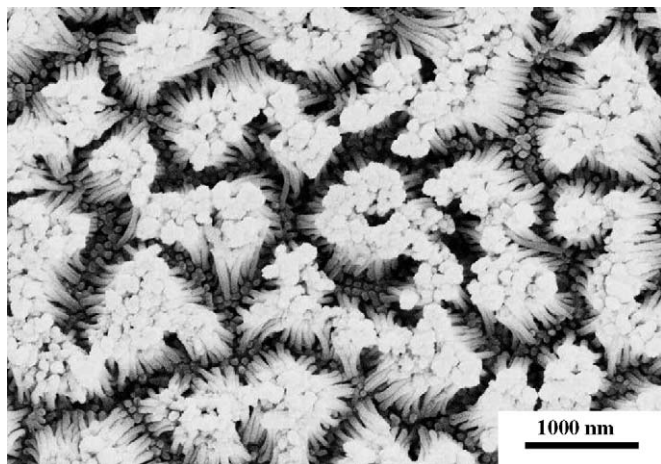


Fig. 2. FESEM image of MnO₂ nanowire arrays grown on AAO/Ti/Si substrate.

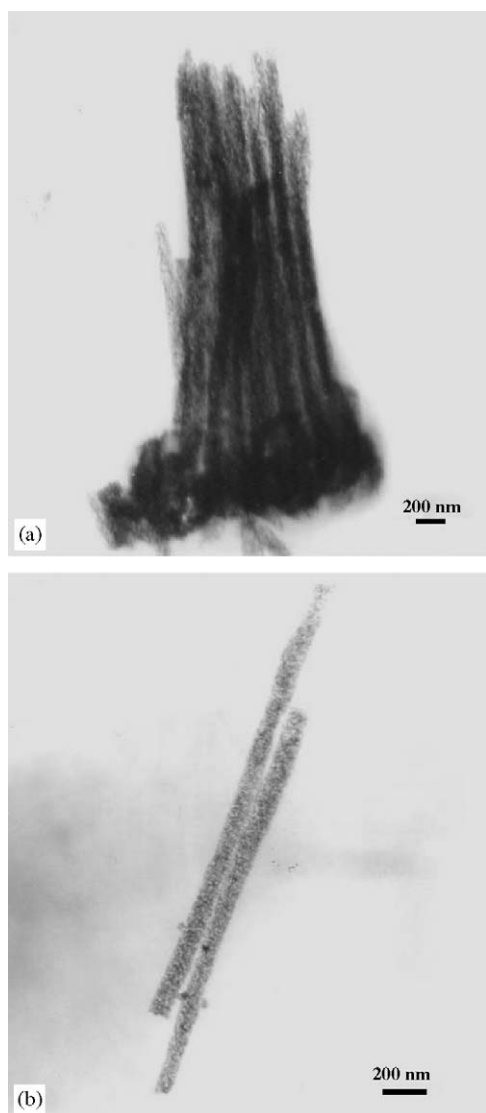


Fig. 3. TEM images of MnO₂ nanowires: (a) truss nanowires, (b) single nanowires.

determined from Fig. 3 to be about 40 nm and 1 μm, respectively. These nanowire diameters are identical to the pore diameters of the AAO template on Ti/Si substrate. From the diameter, filling rate and the length of the nanowires it is easy to show that the nanowire array electrode have 11 cm² of MnO₂ area per cm² of substrate electrode area.

Fig. 4 illustrates the XRD patterns of the samples heat-treated at different temperatures up to 400 °C. The main peaks of the α-MnO₂ [34] can be roughly identified in Fig. 4. However, the amorphous nature of the samples is confirmed by the XRD spectrum, which shows broad and low intense peaks related to a poorly crystallized compound. The amorphous nature is still retained for the material heat-treated at 400 °C.

Fig. 5 shows the TG–DTA curves of the as-prepared sample. The first weight loss at 35–104 °C results from the removal of physically absorbed water, the second step weight loss at 104–252 °C is the removal of chemically bound water in the samples, and the third step weight loss are due to the structure transformation. DTA displays two obvious exothermic peaks at 206 and 513 °C, which correspond to the removal of chemically bound water and the transition of MnO₂ to Mn₂O₃ as determined by Reddy [35], respectively.

Typical cyclic voltammograms of the samples heat-treated at different temperatures for 2 h measured in 0.5 M Na₂SO₄ at 5 mV/s scan rate are shown as curves (a), (b) and (c) in Fig. 6. Within the potential range –0.1 to 0.9 vs. SCE, the capacitive-like and symmetric *I/E* responses of the CV curves indicate that the oxides through different temperature treatments exhibit electrochemical characteristics suitable for pseudocapacitor application. But only the sample obtained at 200 °C has the ideal regular rectangle, as shown in curve (b). It is ascribed to the variation of crystalline water content as depicted in the literature [24].

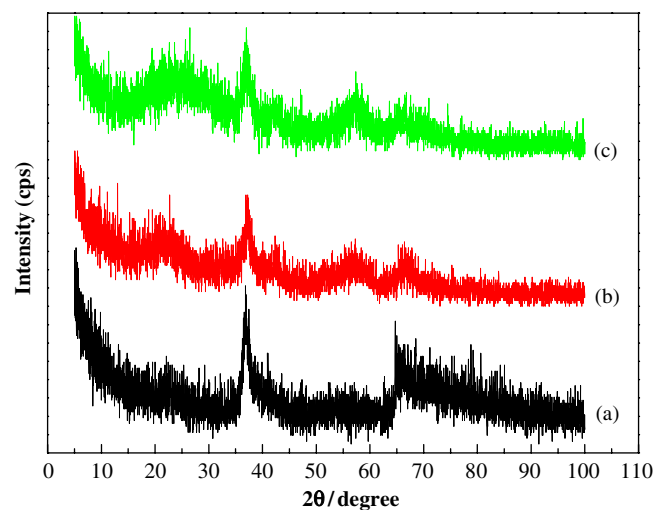


Fig. 4. XRD patterns of the samples heat-treated at different temperatures for 2 h: (a) as-prepared, (b) heat-treated at 200 °C, (c) heat-treated at 400 °C.

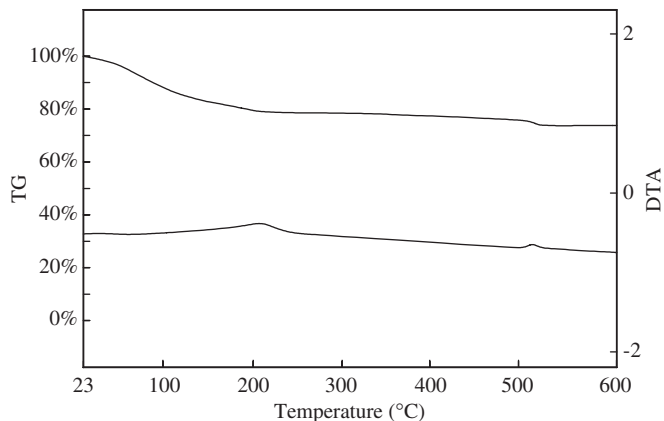


Fig. 5. TG and DTA curves for as-prepared sample. Heating rate: 10 °C/min.

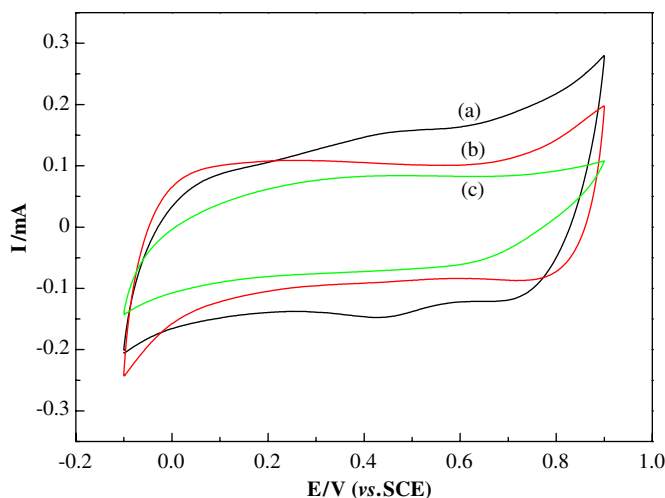


Fig. 6. CV curves of the samples heat-treated at different temperatures for 2 h at 5 mV/s scan rate: (a) as-prepared, (b) heat-treated at 200 °C, (c) heat-treated at 300 °C.

The results indicate that the sample heat-treated at 200 °C has the ideal capacitive behaviors for electrochemical capacitors.

Fig. 7 shows the CV curves of the sample heat-treated at 200 °C at different scan rates. Note that the shape of these voltammetric curves is not significantly influenced by the change in scan rate of CV. In addition, voltammetric currents are directly proportional to the scan rate of CV. These results indicate ideal capacitive behavior of the nanowire arrays heat-treated at 200 °C. Because the prepared nanowire arrays possess high surface area and high aspect ratio, the interface between the active material and electrolyte increase. The specific capacitance of the sample heat-treated at 200 °C at 10 mV/s scan rate is 254 F/g, which can be estimated from the cyclic voltammogram according to the following equation [34]:

$$C_{cv} = \frac{Q}{\Delta E \times m},$$

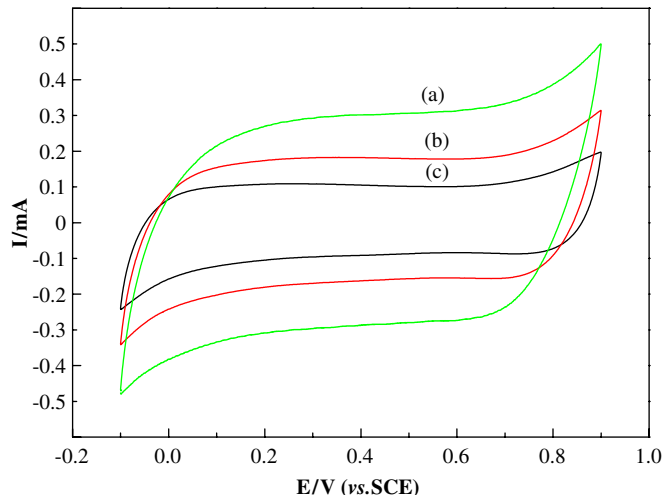


Fig. 7. CV curves of the samples heat-treated at 200 °C at different scan rates: (a) $V = 20$ mV/s, (b) $V = 10$ mV/s, (c) $V = 5$ mV/s.

where C_{cv} is the specific capacitance (in F/g), Q is the charge (in C), ΔE is the potential window (in V), and m is the mass of active material (in g). The above results demonstrate that the prepared MnO_2 nanowire array thin films on Ti/Si substrate in 0.5 M Na_2SO_4 aqueous electrolyte can be as an excellent electrode for electrochemical capacitor.

4. Conclusion

In this work, MnO_2 nanowire arrays were electrodeposited in AAO template on Ti/Si substrate. The AAO/Ti/Si substrate had unique electrodeposition properties and could bond well with the deposited materials. XRD analysis indicated that the synthesized sample had amorphous nature until 400 °C. The MnO_2 nanowire array electrode heat-treated at 200 °C showed ideal capacitive behavior and the specific capacitance can be up to 254 F/g. So it had promising application in electrochemical capacitor.

Acknowledgments

This work is supported by the National Natural Science Foundation of China (NNSFC60471014).

References

- [1] E. Frackowiak, F. Béguin, Carbon 39 (2001) 937–950.
- [2] C. Lin, B.N. Popov, H.J. Ploehn, J. Electrochem. Soc. 149 (2002) A167–A175.
- [3] D. Villers, D. Jobin, C. Soucy, D. Cossement, R. Chahine, L. Breau, D. Béllanger, J. Electrochem. Soc. 150 (2003) A747–A752.
- [4] F. Fusalba, N. El Mehdi, L. Breau, D. Béllanger, Chem. Mater. 12 (2000) 2581–2589.
- [5] J.I. Hong, I.H. Yeo, W.K. Paik, J. Electrochem. Soc. 148 (2001) A156–A163.
- [6] P. Soudan, J. Gaudet, D. Guay, D. Béllanger, R. Schulz, Chem. Mater. 14 (2002) 1210–1215.

- [7] B.E. Conway, V. Birss, J. Wojtowicz, J. Power Sources 66 (1997) 1–14.
- [8] P.A. Nelson, J.R. Owen, J. Electrochem. Soc. 150 (2003) A1313–A1317.
- [9] C. Lin, J.A. Ritter, B.N. Popov, J. Electrochem. Soc. 145 (1998) 4097–4103.
- [10] N.L. Wu, S.Y. Wang, C.Y. Han, D.S. Wu, L.R. Shiue, J. Power Sources 113 (2003) 173–178.
- [11] N.L. Wu, Mater. Chem. Phys. 75 (2002) 6–11.
- [12] T. Brousse, D. Béllanger, Electrochem. Solid-State Lett. 6 (2003) A244–A248.
- [13] H.Y. Lee, J.B. Goodenough, J. Solid State Chem. 144 (1999) 220–223.
- [14] S.C. Pang, M.A. Anderson, T.W. Chapman, J. Electrochem. Soc. 147 (2000) 444–450.
- [15] H.Y. Lee, S.W. Kim, H.Y. Lee, Electrochem. Solid-State Lett. 4 (2001) A19–A22.
- [16] C.C. Hu, T.W. Tsou, Electrochem. Commun. 4 (2002) 105–109.
- [17] S.F. Chin, S.C. Pang, M.A. Anderson, J. Electrochem. Soc. 149 (2002) A379–A384.
- [18] M. Toupin, T. Brousse, D. Béllanger, Chem. Mater. 14 (2002) 3946–3952.
- [19] T. Brousse, M. Toupin, D. Béllanger, J. Electrochem. Soc. 151 (2004) A614–A662.
- [20] J. Jiang, A. Kucernak, Electrochim. Acta 47 (2002) 2381–2386.
- [21] C.C. Hu, T.W. Tsou, Electrochim. Acta 47 (2002) 3523–3532.
- [22] Y.U. Jeong, A. Manthiram, J. Electrochem. Soc. 149 (2002) A1419–A1422.
- [23] J.N. Broughton, M.J. Brett, Electrochem. Solid-State Lett. 5 (2002) A279–A282.
- [24] H. Kim, B.N. Popov, J. Electrochem. Soc. 150 (2003) D56–D62.
- [25] C.C. Hu, C.C. Wang, J. Electrochem. Soc. 150 (2003) A1079–A1084.
- [26] J.K. Chang, W.T. Tsai, J. Electrochem. Soc. 150 (2003) A1333–A1338.
- [27] R.N. Reddy, R.G. Reddy, J. Power Sources 124 (2003) 330–337.
- [28] N. Li, C.R. Martin, B. Scrosati, Electrochem. Solid-State Lett. 3 (2000) 316–318.
- [29] N. Li, C.R. Martin, B. Scrosati, J. Power Sources 240 (2001) 97–98.
- [30] C.J. Patrissi, C.R. Martin, J. Electrochem. Soc. 146 (1999) 3176–3180.
- [31] W.C. West, N.V. Myung, J.F. Whitacre, B.V. Ratnakumar, J. Power Sources 126 (2004) 203–206.
- [32] Y.F. Mei, X.L. Wu, X.F. Shao, G.S. Huang, G.G. Siu, Phys. Lett. A 309 (2003) 109–113.
- [33] M.S. Sander, L.S. Tan, Adv. Funct. Mater. 13 (2003) 393–397.
- [34] M. Toupin, T. Brousse, D. Béllanger, Chem. Mater. 16 (2004) 3184–3190.
- [35] R.N. Reddy, R.G. Reddy, J. Power Sources 132 (2004) 315–320.